iJRASET
International Journal For Research in Applied Science and Engineering Technology

INTERNATIONAL JOURNAL FOR RESEARCH

IN APPLIED SCIENCE & ENGINEERING TECHNOLOGY

Volume: 13 **Issue:** IV **Month of publication:** April 2025

DOI: https://doi.org/10.22214/ijraset.2025.68155

www.ijraset.com

Call: 08813907089 | E-mail ID: ijraset@gmail.com

International Journal for Research in Applied Science & Engineering Technology (IJRASET)
ISSN: 2321-9653; IC Value: 45.98; SJ Impact Factor: 7.538
Volume 13 Issue IV Apr 2025- Available at www.ijraset.com

Fuzzy Logic-Driven Power Management Algorithm (PMA) for Grid-Tied PV System with Hybrid Energy Storage

U. Sreenivas[1], K. Ashrafulla Khan[2], M. Jyothsna[3], G. Chandrika[4], G. Govardhan Reddy[5], S. Harshitha[6]
[1]*Professor Department of EEE, Srinivasa Ramanujan Institute of Technology, Anantapur, India*
[2, 3, 4, 5, 6]*Student, Department of EEE, Srinivasa Ramanujan Institute of Technology, Anantapur, India*

Abstract: ***This project proposes a fuzzy logic-based power management algorithm (PMA) for integrating grid-tied photovoltaic (PV) systems with a hybrid energy storage. The proposed algorithm's stated goals include improving the grid's stability and dependability, and making better utilization of renewable energy. The suggested control scheme allows for efficient regulation of power flow and optimizes self-consumption for PV energy through successfully coordinating the photovoltaic system, grid, with hybrid energy storage. Aiming to maximize power management, the fuzzy logic controller takes into account an assortment of input factors, including PV output, energy storage state-of-charge, and grid demand. These scheme's efficacy in integrating renewable energy sources, decreasing grid reliance, and guaranteeing a steady power supply is shown by the simulation results.***
Keywords: Grid-tied photovoltaic (PV) system, Microgrid, Power management algorithm (PMA), Hybrid energy storage (HES), Super-capacitor.

I. INTRODUCTION

As a result of rising awareness of the need to reduce energy use and the fast elaboration of green energy sources, modern power system places a premium on environmentally friendly technology. These days, wind turbines with photovoltaic (PV) systems are the greenest technology on the market. Due to its many benefits, including inexpensive, more effectual, maintenance free, and high consistency, PV offers most reliable and sustainable option. The linked system's stability is adversely impacted by the fluctuating environmental operating circumstances, which include temperature, irradiance, partial shading effects, and humidity, and these have strongest impact on longevity and generation output of PV. To improve the system's quality and stability, microgrids use energy storage systems (PSSs) to reduce power mismatch between produced and needed power, increase the system's reliability, and deliver continuous power via intermittent sources like PV. Because of its simplicity and widespread usage, the battery has become the go-to energy storage device. Nevertheless, due to their moderate power density and high energy density, batteries provide sluggish charging and discharging speeds. In contrast to batteries, which allow for rapid charging and discharge, super-capacitors possess low energy storage and instantaneous power supply. The combined use of a battery with a super capacitor allows for the creation of hybrid energy storage systems (HESSs), that combines advantages related to both technologies. Using HESS, the transient current from the batteries flows to the super capacitors, extending the life of any batteries [2]. With the hybrid microgrid to work efficiently and without hitches, a plan for correct power monitoring is required. Among the services that the strategy should offer are controlling the centralized power supplied by every distributed generator (DG), monitoring the system's frequency as well as voltage, ensuring that generation and demand are balanced, providing cost-effective power, regulating voltages across the DC link, improving power quality, smoothly transitioning to operation, and keeping energy storage devices' state of charge (SOC) inside their limits [3].

II. FRAMEWORK AND POWER MANAGEMENT TECHNIQUE

The framework of fuzzy logic-driven power management algorithm for grid-tied PV system with hybrid energy storage is described in Fig.2.1, where the framework incorporates of photovoltaic (PV) cell, quadratic boost converter, battery, super-capacitor, LC filter, DC-DC converters, voltage source converter (VSC), RL load and non-linear load. The primary renewable energy source for the system is from photonic array which transforms the solar energy into usable electricity, it generates DC electricity but the output of PV is fluctuating voltage it is due to fluctuations in solar radiation. The generated DC power of PV array is fed into quadratic boost converter, boost up output voltage of PV from lower to higher level to get required DC link voltage and makes extraction of power effectively and supplies stable power. The DC voltage from DC link which is stabilized fed to DC link which is the central energy part related to framework.

©IJRASET: All Rights are Reserved

Then stabilized direct current voltage of DC link is fed to voltage source converter which converts into AC, before sending the AC output to utility grid, an LC filter is connected to remove harmonics which are high received from voltage source converter by the switching operations. This LC filter smooth the current and voltage waveforms at AC side. In the system RL load and non-linear load both are associated with the proposed system to check its performance under different operating conditions.

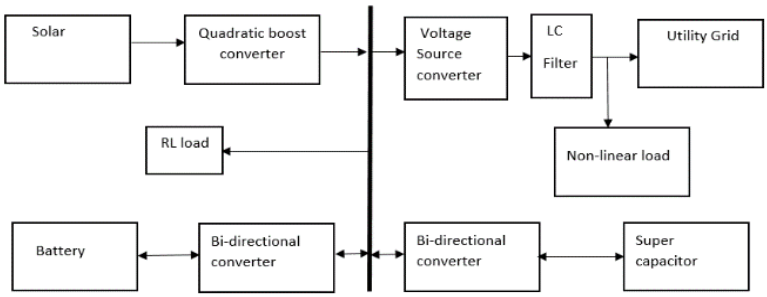

Fig.2.1. Framework of grid-tied photovoltaic system integrated with hybrid energy storage system

Whereas hybrid energy storage incorporates battery and super-capacitor where a separate bi-directional DC-DC converter connected battery which enables transfer power via battery and DC link. Here battery stores energy for long term and supply energy to system by discharging when there is shortage of power. And a separate bi-directional DC-DC converter connected via super-capacitor enables transfer power via super-capacitor and DC link, where super-capacitor supplies stable supply under the varied load and variation in generation and also responds quickly to transient fluctuations. Bi-directional DC-DC converters connected to battery together with super-capacitor controls the discharging and charging, thereby enabling the optimized power distribution between energy storage components and the DC link.

A. Power control technique

The Fig.2.2 illustrates the power control technique developed for integrating a photovoltaic system with the grid using a hybrid energy storage system. This system maintains DC link voltage stable and provides effectual power distribution, and supply power flow properly among different sources and loads. First it determines the error by comparing reference and actual dc voltage at DC link. The error determined by the fuzzy logic controller helps maintain a stable DC voltage by dynamically adjusting control actions. The output of fuzzy logic controller is fed into low-pass filter where transient variations are smoothed out before further processing. The λ-block ensures optimal power distribution and generates control parameters for power balancing. It also estimates the state of charge (SOC_b) of battery and ensures operation within predefined higher and lower limits.

A mode selector which dynamically adjust power allocation by processing inputs such as battery current (i_b), grid reference current (i_{gr}) and generated power (P_t) and as per available PV power, state-of-charge of battery (SOC_b) and grid demand determines the priority of power flow. The PMA module which calculates current reference for different components like super-capacitor current reference ($I_{sc(ref)}$), battery current reference ($I_{b(ref)}$), grid current reference ($I_{g(ref)}$). These current references enhance the stability and efficiency of the system by assuring a proper power distribution among the battery, PV system, super-capacitor and grid.

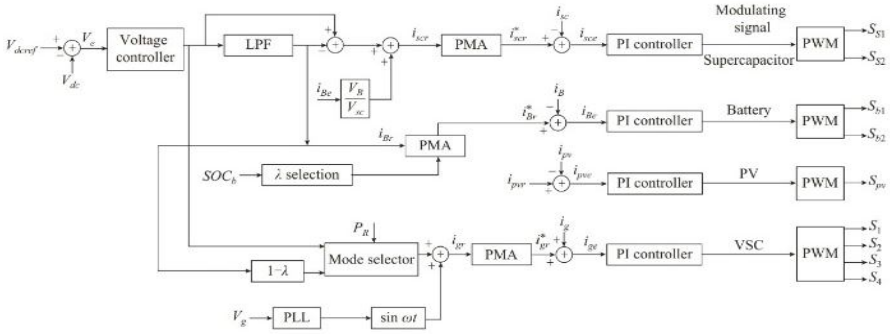

Fig.2.2. Proposed Power management technique

The reference values attained from PMA module are used to regulate power flow through PI controllers. Where the PI controller of super-capacitor regulates it charging and discharging cycles and PI controller of battery controls the energy transfer between battery and the system and PI controller of PV maximizes power extraction from solar radiation and PI controller of grid supplies stable power to the grid. The outputs of the PI controller from various components are fed into the Pulse Width Modulation (PWM) system, which generates switching signals for power converters. These signals regulate power flow to the super-capacitor, battery, solar PV, and voltage source converter.

B. Power Management Algorithm (PMA)

The system's operating state, selected by the PMA, is determined by the available power output and the load power. Three operational power modes (PR modes) have been identified. Where PR calculated as follows

$$P_R = P_l - P_{PV} \quad (1)$$

The three power modes are (i) Insufficient Power Mode (IPM): PR value is greater than zero, (ii) Sufficient Power Mode (SPM) where PR value is less than zero and (iii) Floating Power Mode (FPM): PR is set to zero. According to the state-of-charge of battery (SOC_b) and state-of-charge of super-capacitor (SOC_{sc}) again these three modes are classified into three operations as per SOC of battery and super-capacitor. Through these classified mode operations, the PMA generates current reference values, which are fed into the PI controller to determine the error. This error is then forwarded to the PWM system, which generates signals for the battery and super-capacitor converters, enabling charging or discharging to achieve power stability at the DC link. The state-of-charge (SOC) is calculated following the Coulomb counting approach, as outlined in Fig.2.3.

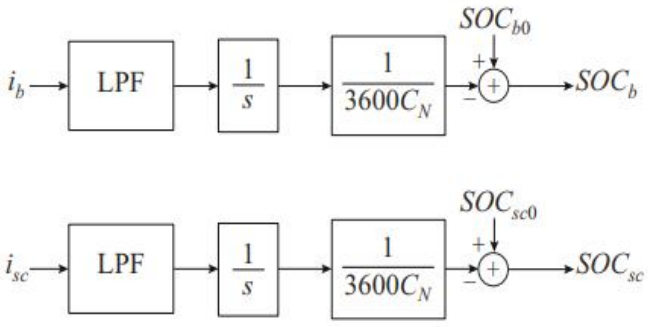

Fig. 2.3. SOC calculation using coulomb counting approach

1) Insufficient Power Mode (IPM):

Under this operating mode, the electricity demand exceeds the capacity of the PV system. Consequently, the main grid, PV, and battery compensate for the average power deficit while ensuring the SOC_b remains within its constraints. Meanwhile, the super-capacitor manages the transient power component until it meets its SOC lower threshold. The transient and oscillatory power is handled by the main grid, battery and super-capacitor, which discharge to supply power to the DC link.

2) Sufficient Power Mode (SPM):

In this mode, whenever the power output from the PV system exceeds the demand, the surplus power is directed to the battery and super-capacitor for charging, following the SOC limit conditions. Upon the battery and super-capacitor reaching their upper SOC limits, the surplus power is transferred to the utility grid via the voltage source converter (VSC).

3) Floating Power Mode (FPM):

Under this operating mode, If the electricity produced by the PV system does not match the load demand i.e., either exceeding or falling short; the storage systems are charged using power from the utility grid. After the storage systems reach full charge, the battery stays idle while the super-capacitor continues supplying transient power as needed.

C. Generation process of current references for grid and HESS

The electrical power between the solar unit and energy storage systems should be balanced, as they are connected to a grid-tied DC microgrid while ensuring stability in the AC utility grid. To maintain system stability, a complete power equilibrium is required. The necessary power equilibrium is:

$P_g(t) + P_{PV}(t) + P_B(t) + P_{SC}(t) - P_l(t) = P_t(t)$ (2)

Where $P_l(t)$ represents the load power which is the sum of DC and AC load powers. That is:

$P_l(t) = P_{ldc}(t) + P_{lac}(t)$ (3)

The equation (2) represents the power from the grid, photovoltaic (PV) system, battery and super-capacitor. The total required power segmented into two components at DC link to maintain power balance. The two components are (i) Average power $P_t(t)$ and (ii) Transient power $P'_t(t)$.

Then the total corresponding current is:

$i_t(t) = V_{dc}P_t(t) + V_{dc}P'_t(t) = i_t(t) + i'_t(t)$ (4)

Where $i_t(t)$, $i'_t(t)$ are the average and transient currents, where DC bus current is regulated using voltage controller.

$i_t(t) = K_{pvd}\, V_e + K_{ivd} \int V_e\, dt$ (5)

where K_{pvd}, K_{ivd} are proportional coefficients and integral coefficients of voltage control loop and V_e is the DC voltage error. $\bar{i}_t(s)$ is the average current extracted by a low pass filter, which is distributed with the PV system, battery and grid. Super-capacitor handled the transient component is

$\bar{i}_t(s) = \frac{\omega_c}{s+\omega_c}\, i_t(s)$ (6)

$i_{Br}(s) = \lambda \bar{i}_t(s)$ (7)

$i_{gr}(s) = (1-\lambda)\bar{i}_t(s)$ (8)

$i'_t(s) = (1 - \frac{\omega_c}{s+\omega_c})i_t(s)$ (9)

III.SIMULATION RESULTS

A. System output under variation in photovoltaic power

The system's performance under varying PV power with constant loads is depicted in Figures 3.1, 3.2, 3.3, 3.4, 3.5, and 3.6. As illustrated in Fig.3.1, the DC link voltage (V_{dc}) stabilizes around 100 V and remains relatively constant throughout the 4-second simulation period. Fig.3.2 illustrates the battery voltage (V_b), where the graph shows a slight decline, indicating the discharging process.

The battery voltage (V_b) starts at approximately 46 V. The Fig.3.3 depicts the voltage graph of the super-capacitor, which remains stable at 50 V, demonstrating its role in supporting the system by providing transient power. Fig.3.4 presents the graph of the grid current, illustrating the stable transfer of power to the grid with consistent alternating waveforms. Fig.3.5 represents the total harmonic distortion (THD), which is 0.41%. This low value confirms that the power quality is high. The Fig.3.6 represents the power flow graphs of PV power (P_{PV}), battery power (P_b), super-capacitor power (P_{SC}) and grid power (P_g). Here, we observe a reduction in PV power after 2 seconds. In this scenario, the battery and super-capacitor work together to supply stable power, demonstrating how the fuzzy logic controller effectively manages power distribution to maintain system stability during PV power fluctuations.

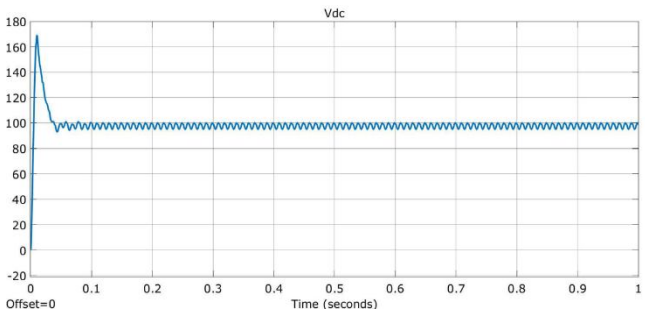

Fig.3.1. DC link voltage (V_{dc}) under variation in photovoltaic power

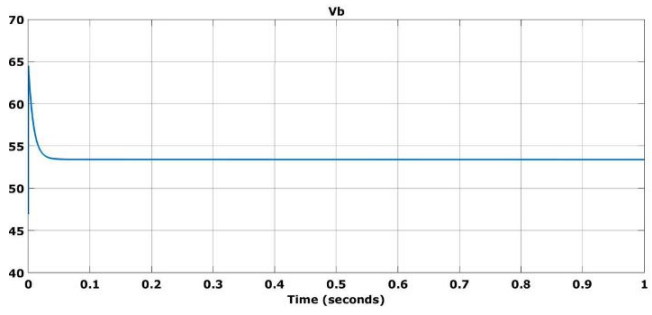

Fig.3.2. Battery voltage (V_b) under variation in photovoltaic power

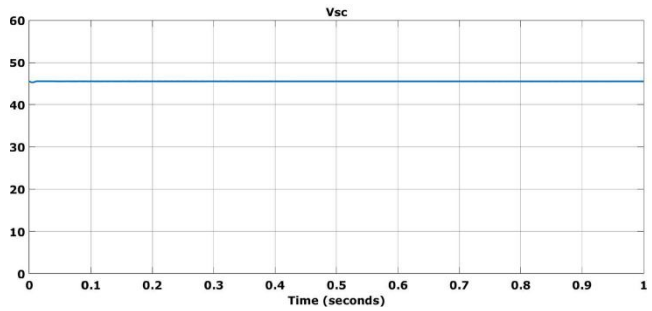

Fig.3.3. Super-capacitor voltage (V_{sc}) under variation in photovoltaic power

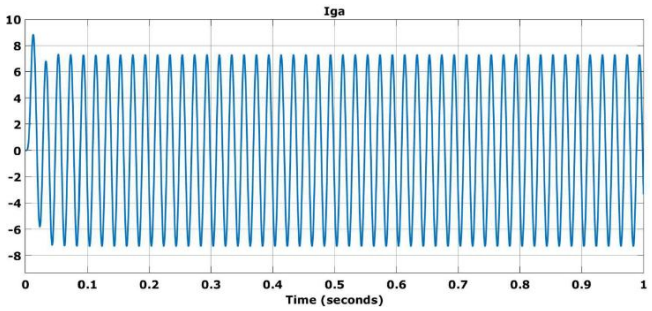

Fig.3.4. Grid current (I_g) under variation in photovoltaic power

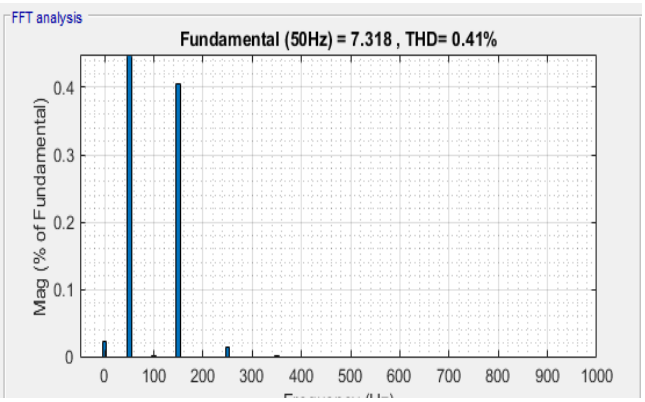

Fig.3.5. The total harmonic distortion (THD) under variation in photovoltaic power

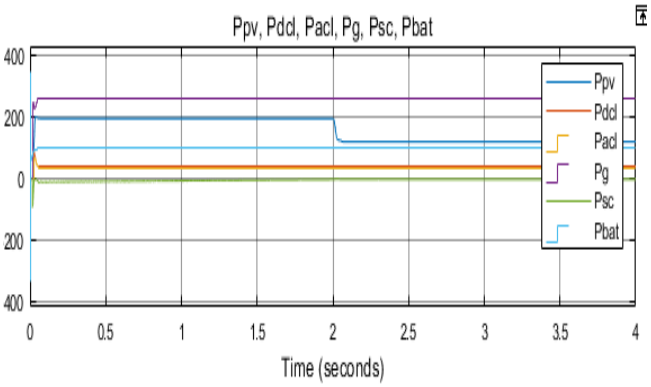

Fig.3.6. Power drawn by DC & AC loads and power outputs of super-capacitor, battery, PV system, and utility grid under variation in photovoltaic power

B. System output under load variation

Under load-varying conditions, the system's performance is illustrated in Figures 3.7, 3.8, 3.9, and 3.10. Fig.3.7 demonstrates the DC link voltage, which is maintained stable at approximately 100 V despite load variations. Fig.3.8 shows the battery voltage (V_b) gradually decreasing, indicating discharging as it supplies power to maintain a stable system. The battery voltage starts at approximately 54 V.

Fig.3.9 represents the super-capacitor voltage (V_{sc}), which remains stable at 46 V, effectively smoothing transient power fluctuations. Fig.3.10 analyzes power flow, where PV power (P_{PV}) remains around 250 W, while storage components and grid power (P_g) dynamically respond to maintain system stability.

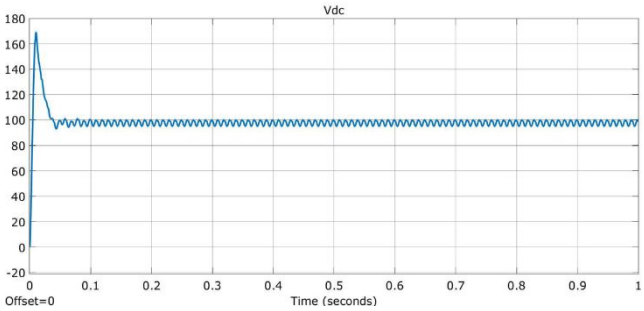

Fig.3.7. DC link voltage (V_{dc}) under variation in photovoltaic power

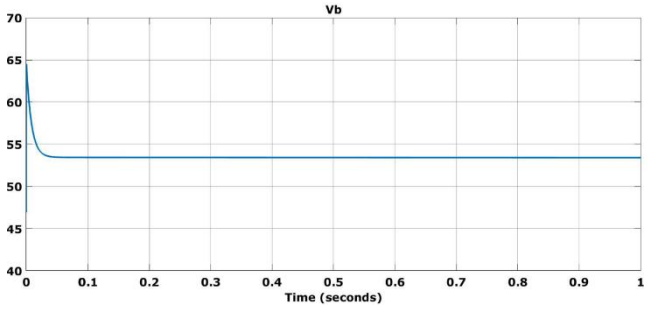

Fig.3.8. Battery voltage (V_b) under variation in photovoltaic power

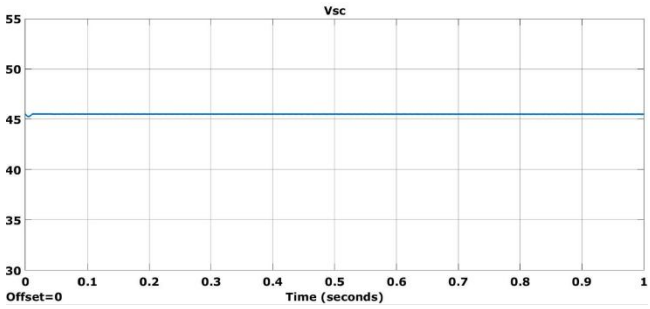

Fig.3.9. Super-capacitor voltage (V_{sc}) under load variation

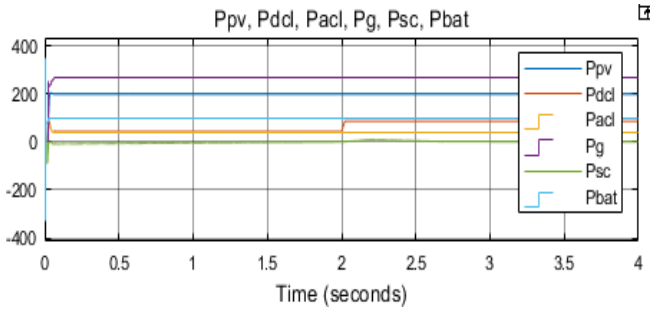

Fig.3.10. Power drawn by DC & AC loads and power outputs of super-capacitor, battery, PV system, and utility grid under load variation

C. System output under Insufficient Power Mode

The system's performance under Insufficient Power Mode (IPM) is illustrated in Figures 3.11, 3.12, 3.13, 3.14, 3.15, and 3.16. Fig.3.11 represents the DC link voltage (V_{dc}), which remains stabilized at 100 V despite lower PV power generation. Fig.3.12 demonstrates the battery voltage (V_b) dropping from 55 V to 52 V, indicating that the battery is discharging to maintain system stability. Fig.3.13 depicts the super-capacitor voltage, which remains stable at 45 V. Fig.3.14 depicts grid voltage and grid current. Fig.3.15 depicts voltage source converter current. Fig.3.16 illustrates PV power fluctuations between 150 W and 200 W, leading to an increased dependency on battery power (P_b) and grid power (P_g) to meet the DC load power (P_{dcl}). Since the super-capacitor charges and discharges quickly, its involvement is minimal in this scenario, making it largely inactive while the system prioritizes battery discharge to maintain energy balance.

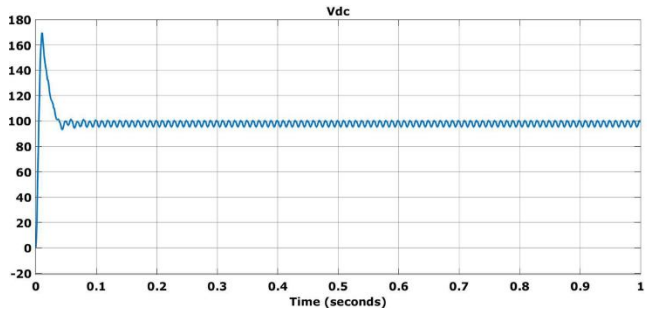

Fig.3.11. DC link voltage (V_{dc}) under variation in IPM

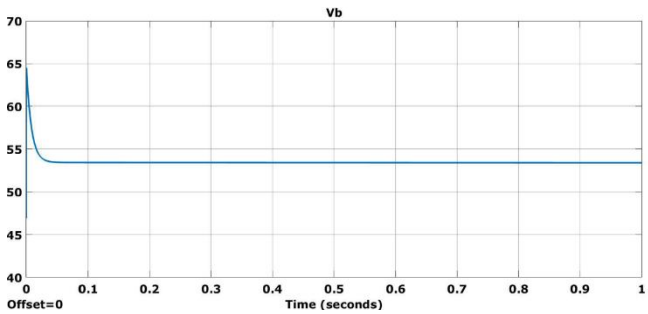

Fig.3.12. Battery voltage (V_b) under variation in IPM

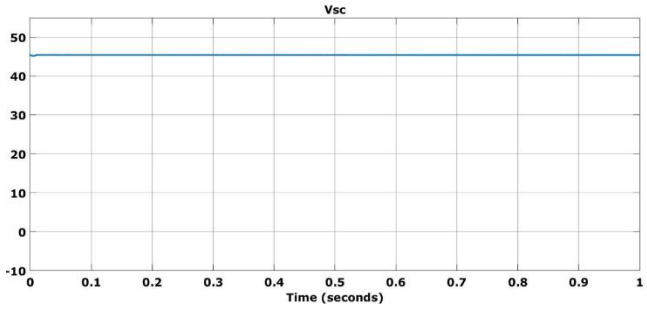

Fig.3.13. Super-capacitor voltage (V_{sc}) under variation in IPM

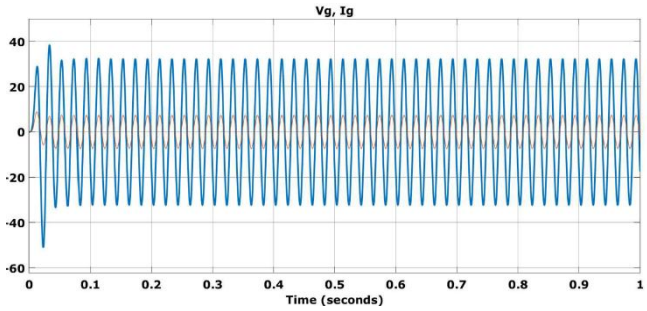

Fig.3.14. Grid voltage (V_g), Grid current (I_g) under variation in IPM

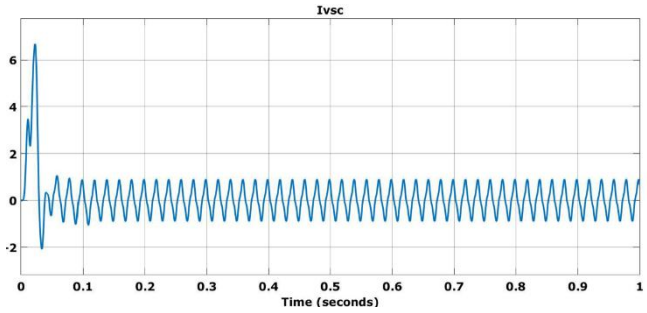

Fig.3.15. Voltage Source Converter current (I_{vsc}) under variation in IPM

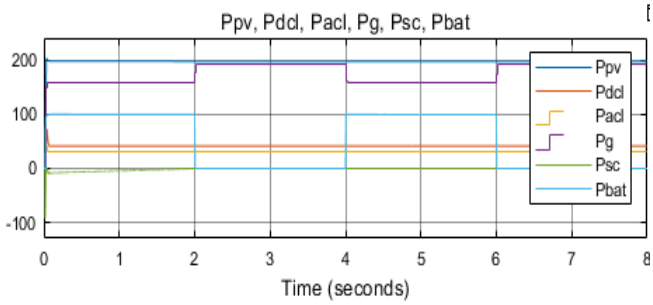

Fig.3.16. Power drawn by DC & AC loads and power outputs of super-capacitor, battery, PV system, and utility grid under IPM.

D. System output under Insufficient Power Mode

The system's performance in Sufficient Power Mode (SPM) is illustrated in Figures 3.17, 3.18, 3.19, and 3.20. Fig.3.17 presents the DC bus voltage (V_{dc}), which is approximately 200 V with slight fluctuations. These variations indicate that the system is actively stabilizing the voltage. Fig.3.18 displays the battery voltage (V_b), which is consistently maintained at 65 V. Fig.3.19 shows the super-capacitor voltage (V_{sc}), which plays a crucial role in compensating transient power fluctuations. It remains stable within the range of 45–50 V, with minimal observed variations. Fig.3.20 illustrates that when the photovoltaic (PV) power adequately supports the load demand, the battery remains inactive, meaning it neither charges nor discharges. Instead, the super-capacitor handles sudden power fluctuations and continuously supplies transient power.

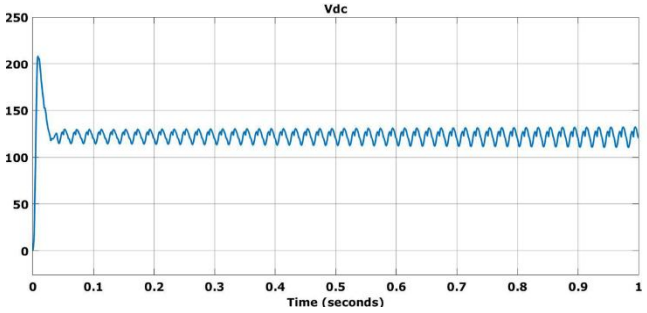

Fig.3.17. DC link voltage (V_{dc}) under variation in SPM

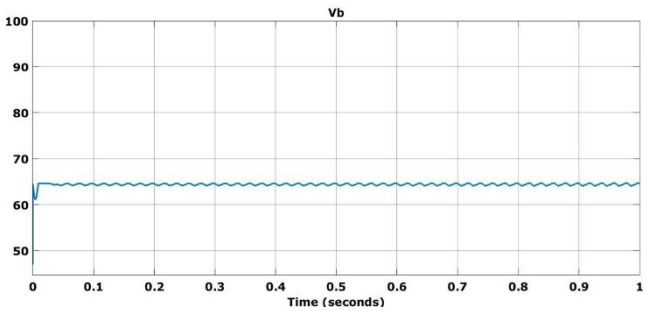

Fig.3.18. Battery voltage (V_b) under variation in SPM

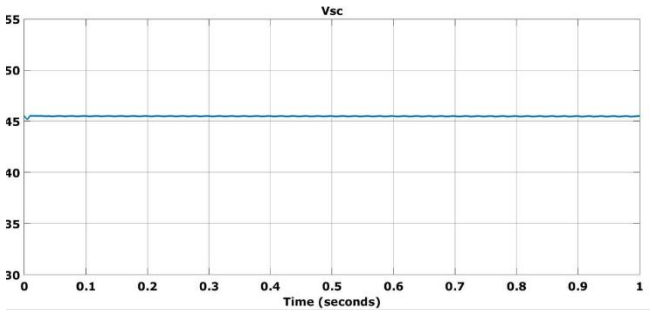

Fig.3.19. Super-capacitor voltage (V_{sc}) under SPM

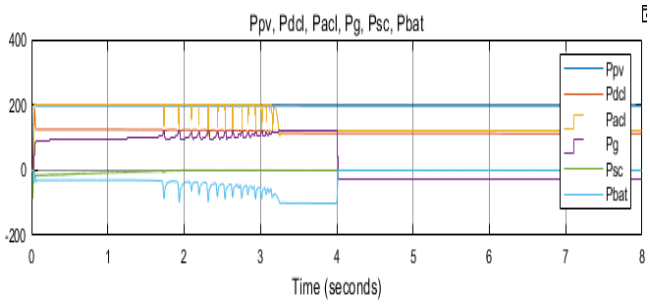

Fig.3.20. Power drawn by DC & AC loads and power outputs of super-capacitor, battery, PV system, and utility grid under SPM

IV. CONCLUSIONS

In conclusion, the fuzzy logic-based power management algorithm with a hybrid energy storage provides an effective solution for challenges associated with grid-tied photovoltaic (PV) integration and energy storage. By combining PV generation with energy storage, the system optimizes power flow, enhancing overall performance and reliability.

The fuzzy logic controller enables real-time adaptive control of the energy storage system's charging and discharging, efficiently handling imprecise and dynamic conditions. As a result, the system improves grid stability, reduces energy costs, and increases resilience by ensuring optimal utilization of available storage capacity and renewable energy sources.

Integrating PV with energy storage offers multiple advantages. Excess energy generated during peak PV output can be stored, reducing reliance on the grid and minimizing energy waste. Conversely, stored energy can be discharged when PV generation is low or demand is high, ensuring a reliable and uninterrupted power supply.

REFERENCES

[1] S. K. Kollimalla and M. K. Mishra, “A novel adaptive P&O MPPT algorithm considering sudden changes in the irradiance,” IEEE Transactions on Energy Conversion, vol. 29, no. 3, pp. 602-610, May 2014.
[2] S. Mishra and R. K. Sharma, “Dynamic power management of PV based islanded microgrid using hybrid energy storage,” in Proceedings of IEEE 6th International Conference on Power Systems (ICPS), New Delhi, India, Mar. 2016, pp. 1-6.
[3] C. Natesan, S. Ajithan, S. Chozhavendhan et al., “Power management strategies in microgrid: a survey,” International Journal of Renewable Energy Research, vol. 5, no. 2, pp. 334-340, Jan. 2015.
[4] Z. Yi, W. Dong, and A. H. Etemadi, “A unified control and power management scheme for PV-battery-based hybrid microgrids for both grid-connected and islanded modes,” IEEE Transactions on Smart Grid, vol. 9, no. 6, pp. 5975-5985, Nov. 2018.
[5] S. Pannala, N. Patari, A. K. Srivastave et al., “Effective control and management scheme for isolated and grid connected DC microgrid,” IEEE Transactions on Industry Applications, vol. 56, no. 6, pp. 1-14, Dec. 2020.
[6] P. Singh and J. S. Lather, “Variable structure control for dynamic power-sharing and voltage regulation of DC microgrid with a hybrid energy storage system,” International Transaction Electrical Energy Sys- tem, vol. 30, no. 9, pp. 1-20, Jun. 2020.
[7] N. R. Tummuru, U. Manandhar, A. Ukil et al., “Control strategy for AC-DC microgrid with hybrid energy storage under different operating modes,” Electrical Power and Energy Systems, vol. 104, pp. 807- 816, Jan. 2019.
[8] J. Hu, Y. Shan, Y. Xu et al., “A coordinated control of hybrid AC/DC microgrids with PV-wind-battery under variable generation and load conditions,” Electrical Power and Energy Systems, vol. 104, pp. 583- 592, Jan. 2019.
[9] H. Mahmood, D. Michaelson, and J. Jiang, “A power management strategy for PV/battery hybrid systems in islanded microgrids,” IEEE Journal of Emerging and Selected Topics in Power Electronics, vol. 2, no. 4, pp. 870-882, Jun. 2014.
[10] P. Sanjeev, N. P. Padhy, and P. Agarwal, “Peak energy management using renewable integrated DC microgrid,” IEEE Transactions on Smart Grid, vol. 9, no. 5, pp. 4906-4917, Sept. 2018.
[11] S. Sahoo, S. Mishra, and N. P. Padhy, “A decentralized adaptive droop-based power management scheme in autonomous DC microgrid,” in Proceedings of IEEE PES Asia-Pacific Power and Energy Conference, Xi’an, China, Dec. 2016, pp. 1018-1022.
[12] P. Singh and J. S. Lather, “Power management and control of a grid-independent DC microgrid with hybrid energy storage system,” Sustainable Energy Technologies and Assessments, vol. 43, pp. 1-11, Feb. 2021.
[13] IEEE Recommended Practice for Utility Interface of Photovoltaic (PV) System, IEEE Standard 929, 2000.
[14] R. Kadri, J. P. Gaubert, G. Champenois et al., “Performance analysis of transformer less single switch quadratic boost converter for grid-connected photovoltaic systems,” in Proceedings of International Conference on Electrical Machines (ICEM), Rome, Italy, Sept. 2010, pp. 1-7.
[15] M. Hamzeh, A. Ghazanfari, Y. A. R. I. Mohamed et al., “Modelling and design of an oscillatory current sharing control strategy in DC microgrids,” IEEE Transactions on Industrial Electronics, vol. 62, no. 11, pp. 6647-6657, Nov. 2015.

[16] B. Singh, D. T. Shahani, and A. K. Verma, "IRPT based control of a 50-kW grid interfaced solar photovoltaic power generating system with power quality improvement," in Proceedings of 4th IEEE International Symposium on Power Electronics for Distributed Generation System (PEDG), Rogers, USA, Apr. 2014, pp. 1-8.
[17] S. Golestan, M. Ramezani, J. Guerrero et al., "Moving average filter-based phase-locked loops: performance analysis and design guide- lines," IEEE Transactions on Power Electronics, vol. 29, no. 6, pp. 2750-2763, Jun. 2014.
[18] N. R. Tummuru, M. K. Mishra, and S. Srinivas, "Dynamic energy management of renewable grid integrated hybrid energy storage sys- tem," IEEE Transactions on Industrial Electronics, vol. 62, no. 12, pp. 7728-7737, Dec. 2015.
[19] H. Wang, Z. Wu, G. Shi et al., "SOC balancing method for hybrid energy storage system in microgrid," in Proceedings of 3rd IEEE International Conference on Green Energy and Applications, Taiyuan, China, Oct. 2019, pp. 141-145.
[20] H. Bindner, T. Cronin, P. Lundsager et al. (2005, Jan.). Lifetime modelling of lead acid batteries. [Online]. Available: https: // www.research-gate.net / publication / 246687286_Lifetime_Modelling_of_Lead_Acid_Batteries.

©IJRASET: All Rights are Reserved | SJ Impact Factor 7.538 | ISRA Journal Impact Factor 7.894 |

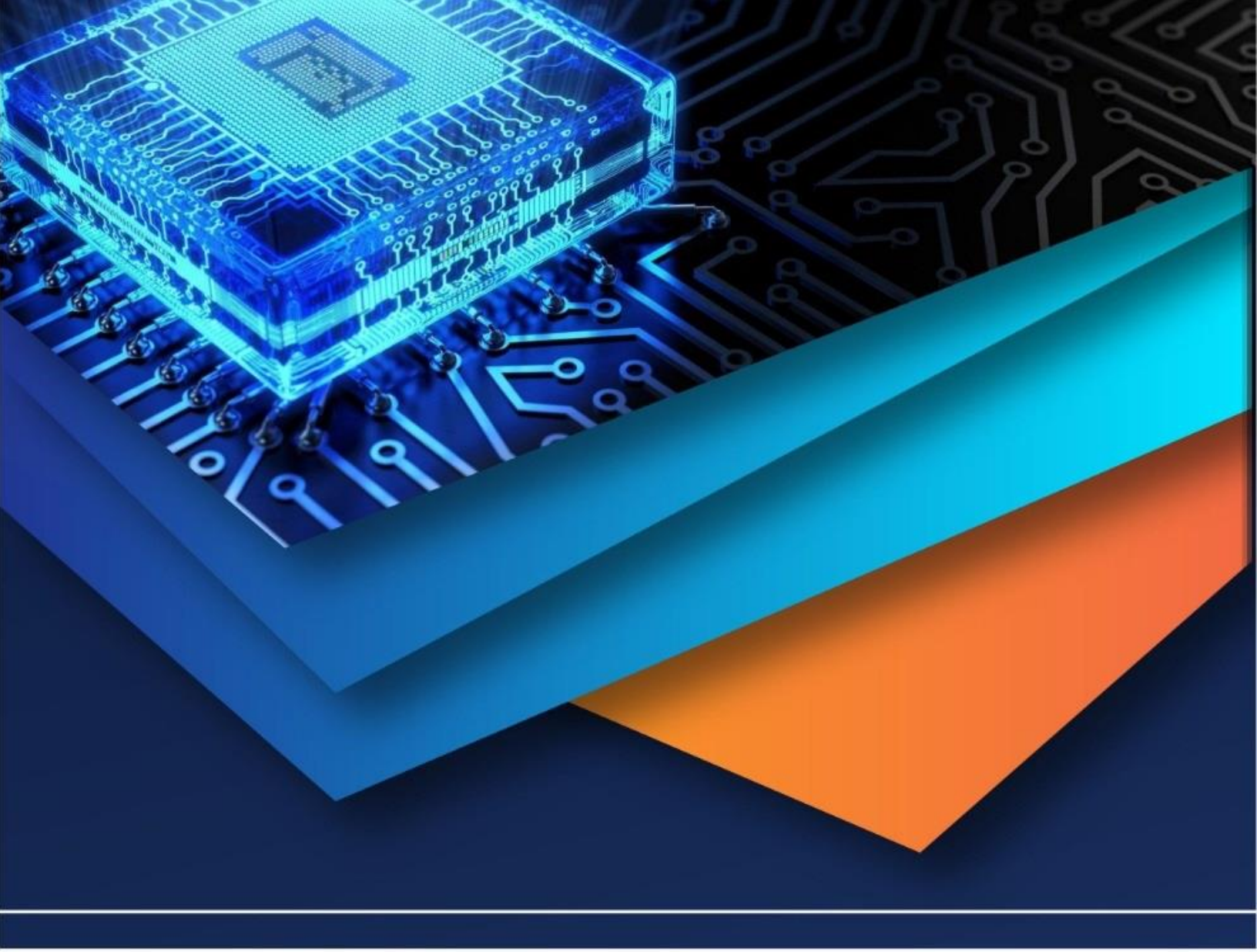

10.22214/IJRASET

45.98

IMPACT FACTOR: 7.129

IMPACT FACTOR: 7.429

INTERNATIONAL JOURNAL FOR RESEARCH

IN APPLIED SCIENCE & ENGINEERING TECHNOLOGY

Call : 08813907089 (24*7 Support on Whatsapp)